RESEARCH ARTICLE

Macromolecular Theory and Simulations
www.mts-journal.de

Intramolecular Hydrogen Bonding in DIBMA Model Compounds

Cornelis A. van Walree

The structure of model compounds for the amphiphilic copolymer poly(diisobutylene-*alt*-maleic acid), DIBMA, is investigated with (gas phase) B3LYP/6-31G and PM7 calculations. It is found that in the monoprotonated state of the repeating unit strong (about 70 kJ mol^{-1}) ionic hydrogen bonds are formed within the hydrogen succinate rings, which impart partial structural rigidity on the backbone of the copolymer. Based on literature pK_a values of the first and second deprotonation step of the succinic acid units, it is argued that the ionic hydrogen bonds are likely to be present in aqueous solution as well. The main chain conformation depends strongly on the stereochemical configuration of the carbon atoms in the hydrogen succinate rings. The possible consequences of the hydrogen bonding for the mechanism of membrane solubilization by maleic acid-based amphiphilic copolymers are discussed.**

1. Introduction

Poly(diisobutylene-*alt*-maleic acid), also known as DIBMA (see **Structure 1**) is an amphiphilic copolymer built from hydrophilic succinate and hydrophobic diisobutylene units. It is obtained by hydrolysis of the copolymer of maleic anhydride and diisobutylene, and is commercially available under the trade name Sokalan CP9. The two types of monomer are present in a 1:1 ratio in an alternating fashion.[1,2]

The interest in DIBMA has increased tremendously in the last years since it was reported that it can be used to prepare disc-shaped lipid bilayer nanoparticles from cell membranes and model systems thereof.[3] This was an important extension to the field in which nanosized lipid particles are made by the use of amphiphilic polymers, in which copolymers of styrene and maleic acid (SMA) play a dominant role.[4–6] SMA is particularly active when possessing styrene to maleic acid ratios of 2:1 (SMA 2:1) and 3:1 (SMA 3:1). The amphiphilic nature of SMA and DIBMA allows to stabilize the nonpolar lipid acyl tails by intercalation of the hydrophobic side groups, while the polar carboxylic acid groups are likely to interact with the polar head groups and the aqueous environment, rendering the nanoparticle soluble in aqueous media.[7,8] In this way, the polymers encircle the lipid particles, forming lipid bilayer discs with diameters of 10–50 nm. With this technique, it is possible to extract membrane proteins along with their native lipid environment.[9,10] This provides an important advantage over other membrane protein isolation methods, like the use of detergents or the combination of detergents and membrane scaffold proteins.

As a function of pH, different charge states are possible for DIBMA. At low pH, both carboxylic groups in the repeating unit are present in the protonated neutral form. At intermediate pH, one COOH group remains, while the other one is deprotonated. At high pH, both groups are present in the anionic COO$^-$-form. DIBMA and SMA are particularly active as a solubilizer of (lipid only) model membranes near pH 7,[11] where the repeating unit is in a monoprotonated state. As insertion is determined by intermolecular interactions and polymer conformation, there might be an optimal charge state at this pH. At low pH, SMA and DIBMA are not soluble in aqueous environment, as amphipathic copolymers of maleic acid adopt a hypercoiled hydrophobic globular conformation.[12] At high pH, there may be too many repulsive electrostatic interactions between polymers and/or lipid head groups.[11] In addition, another conformation is likely to be adopted[13] which also might play a role. For biological membranes, the optimal pH for solubilization may be around 9, though, as was found for *Escherichia coli* membranes.[14] This is related to the presence of proteins, of which the extramembranous parts thwart binding of the polymer to the membrane at physiological pH.

The first step in the formation of nanodiscs is the binding of the amphiphilic polymer to the surface of the lipid bilayer surface. This process is driven by a combination of hydrophobic and electrostatic interactions.[15,16] Subsequently the membrane is perturbed and destabilized by the insertion of the lipophilic side chains, after which the nanodisc is formed. It has been suggested that this occurs via the formation of small, water-filled

C. A. van Walree
Membrane Biochemistry and Biophysics
Utrecht University
Padualaan 8, Utrecht 3584 CH, Netherlands
E-mail: c.a.vanwalree@uu.nl
C. A. van Walree
University College Utrecht
Campusplein 1, Utrecht 3584 ED, Netherlands

The ORCID identification number(s) for the author(s) of this article can be found under https://doi.org/10.1002/mats.202200042

DOI: 10.1002/mats.202200042

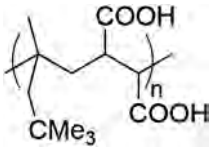

Structure 1.

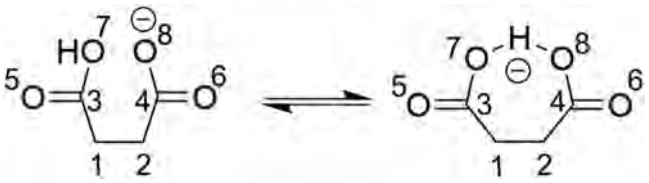

Figure 1. Hydrogen bonding in hydrogen succinate, together with the adopted atom numbering scheme.

pores.[16,17] Orekhov et al. put the idea forward that 2:1 SMA copolymers induce pores, whereas 3:1 SMA copolymers extract lipid patches from the membrane.[18] Pore formation has recently been observed during the formation of nanodiscs with DIBMA.[2]

In this contribution, the structure of DIBMA is explored with the use of density functional and PM7 semi-empirical calculations on low molecular weight model compounds. The structures of the dimer (a single repeating unit of the copolymer), the trimer (1.5 repeating units), the tetramer (2 repeating units), and the pentamer (2.5 repeating units) are investigated (**Scheme 1**). Note that this terminology is different from that used in a paper on the structure of SMA model compounds, where a single repeating unit is referred to as a monomer.[13] Only structures in which one carboxylic acid per repeating unit is deprotonated are considered. In particular, two issues are addressed. These are i) the occurrence of hydrogen bonding between the protonated and deprotonated carboxylic acid groups and ii) the effect of the stereochemical configuration of the chiral atoms in the polymer main chain on its conformation. Finally, possible consequences of the hydrogen bonding for the mechanism of membrane solubilization by maleic acid-based amphiphilic copolymers are discussed.

For the hydrogen succinate anion and the dimer, DFT calculations were run with both the B3LYP and ωB97XD functionals.[19] The ωB97XD method should explicitly take dispersion forces into account and performs well for ionic interactions and charged hydrogen bonds.[20] Although bond lengths and differences in heats of formation differed somewhat with respect to the B3LYP/6-31G** method, the ωB97XD functional was found to give a qualitatively very similar picture. Therefore, ωB97XD/6-31G** results are only reported for the hydrogen succinate ion, but not for the dimer and longer DIBMA model compounds. The PM7 method was predominantly used for the calculation of torsion coordinates.

2. Results

2.1. Hydrogen Bonding in the Hydrogen Succinate Anion

During preliminary calculations on the DIBMA model compounds, it turned out that the hydrogen succinate ring systems in these compounds form cyclic, hydrogen-bonded structures (**Figure 1**). This intramolecular hydrogen bond is first investigated here for hydrogen succinate. In order to assess the strength of the hydrogen bond, both an unbridged, linear structure and a bridged cyclic structure were calculated. The results are listed in **Table 1**.

In the linear geometry, the C4C2C1C3 dihedral angle is about −165° for the DFT structures, while with PM7 an angle of 172.8° is obtained. In the hydrogen-bonded geometries, the dihedral angle is 77–78° in the DFT structures, and 85.8° for PM7. The energy of the open geometries is much higher than that of the H-bonded ones. The difference is 61.3 kJ mol^{-1} for PM7 and as

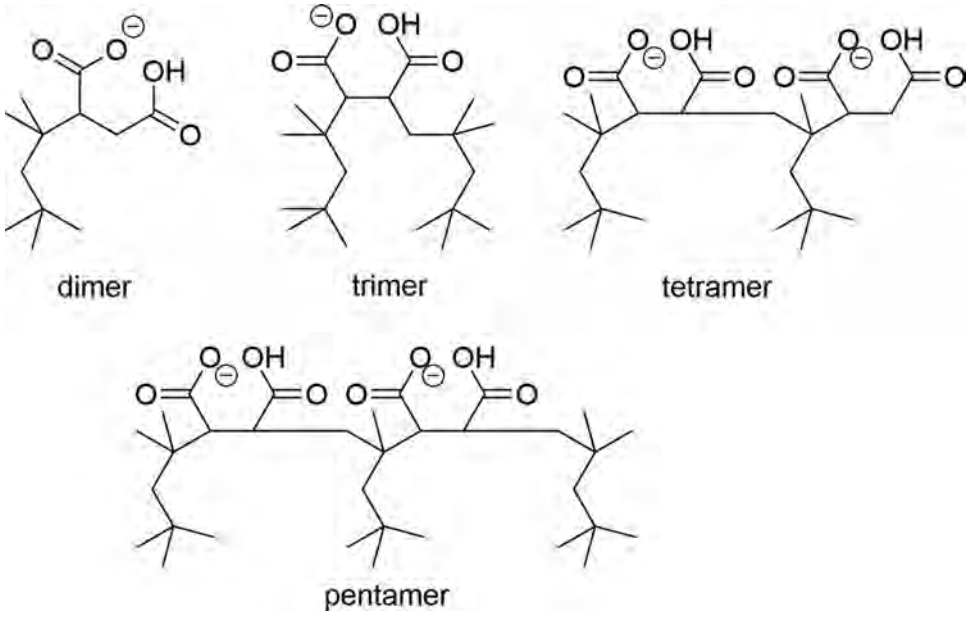

Scheme 1. Structures of the compounds under investigation.

Table 1. Calculated data for hydrogen succinate in the open and H-bonded form. For atom numbering see Figure 1.

Method	H-bond	C4C2C1C3 [°]	E [kJ mol^{-1}]	O7–H[a)] [Å]	O8–H[a)] [Å]	O7–H–O8[b)] [°]	q O7[c)]	q O5[c)]	q O6[c)]	q O8[c)]
B3LYP	no	−164.9	−1198289.43	0.97			−0.4896	−0.5143	−0.6215	−0.6312
B3LYP	yes	76.9	−1198374.57	1.17	1.25	177.4	−0.5907	−0.5561	−0.6124	−0.5684
ωBD97XD	no	−165.3	−1197924.71	0.97			−0.5054	−0.5234	−0.6370	−0.6454
ωBD97XD	yes	78.0	−1198011.01	1.11	1.32	176.5	−0.5889	−0.5571	−0.6426	−0.5876
PM7	no	172.8	−952.89	0.98			−0.6036	−0.5617	−0.7688	−0.7547
PM7	yes	85.8	−1014.23	1.24	1.24	166.1	−0.7019	−0.6458	−0.6457	−0.7013

[a)] Bond length; [b)] Bond angle; [c)] Mulliken charge.

much as 85.1 (B3LYP) and 86.3 (ωB97XD) kJ mol^{-1} for the DFT methods. This difference in energy between the linear and cyclic structure can be taken as the strength of the hydrogen bond, provided that the ring strain is small.[21] For the seven-membered cyclic hydrogen bridged system under consideration here this is indeed the case.[21] Guo et al.[22] arrived at a hydrogen bond strength of 71 kJ mol^{-1} for hydrogen succinate using MP2/6-31++G** calculations. The strength of the hydrogen bond in the hydrogen succinate ion, which is almost as strong as a covalent bond, places it in the category of strong ionic hydrogen bonds.[21,23] It is clear that the attraction of the hydrogen atom to an oxygen bearing a full formal negative charge is much stronger than in the case of a hydrogen bond in which the oxygen atom does not carry a full formal negative charge.

Also other features are similar to that of other strongly hydrogen bonded systems. In the PM7 calculated structure, the O7···H and O8···H bond lengths are equal, as are the Mulliken charges on O7 and O8 (Table 1). This suggests complete sharing of the bridging hydrogen between the two oxygen atoms. The O···H···O angle is 166.1°, close to the preferred linear geometry for hydrogen bonds. With the DFT methods, small differences in the O7···H and O8···H distances and O7 and O8 charges are found, indicating that hydrogen sharing is still very pronounced, but not as complete as in the PM7 case. On the other hand, the O···H···O angle is even closer to 180°. It is noteworthy that although the O7···H and O8···H bond lengths vary for the three methods in all cases the O···O distance is about 2.45 Å. This very short O···O distance also is an indication (albeit not necessarily[24]) of the strength of the hydrogen bond.[23] The charges as well indicate sharing of the hydrogen atom and electron density. When comparing the linear with the cyclic structures, a substantial amount of negative charge has been redistributed from atom O8 to atom O7.

Strong intermolecular ionic hydrogen bonding in hydrogen succinates has been revealed previously by X-ray diffraction studies.[25–27] The anion forms infinite linear chains through hydrogen bonding with short O···O distances of about 2.45 Å, which matches the presently calculated O···O distances. An intramolecular hydrogen bond with O···O distances between 2.41 and 2.45 Å has been reported for the X-ray structures of the monoanion of (±),α,α'-di-*t*-butylsuccinic acid, which was claimed to exhibit the strongest H-bond ever.[28] Strong intramolecular hydrogen bonding in hydrogen succinate was also shown to occur in aprotic solvents and in the gas phase, as revealed by NMR-spectroscopy and computational methods.[22,29,30]

It is of interest to mention that the hydrogen atom in a hydrogen bond can be located exactly in between the two oxygen atoms, or closer to one of the two oxygen atoms.[23,24] In the former case the hydrogen transfer (O···H···O) coordinate possesses a single minimum, in the latter it is a double well potential with a low barrier. Another way to describe the latter type is by tautomerism. Such a double well coordinate can be symmetric or asymmetric. For the intramolecular hydrogen succinate case, NMR studies indicated that the bridging hydrogen atom is subject to a double well potential and proton tautomerism; the potential may become asymmetric as a result of the presence of a solvent.[22,24,28,30] The distance between the two minima was found to be small, ca. 0.2 Å.

It is seen from the results in Table 1 that the DFT methods indeed predict the bridging hydrogen atom to be located nearer to one of the oxygen atoms, and not in the center. Under the assumption that the potential is symmetric, from the O–H bond lengths an off-center distance of 0.04 (B3LYP) and 0.105 (ωB97XD) Å is calculated. It has been argued[24,28] that in solution the asymmetry is caused by local differences in environment of the two hydrogen bonding sites, which cannot be the case for the present gas phase calculations. However, as no symmetry constraints were imposed there are small geometry differences between the two carboxylate groups. In contrast, PM7 predicts the hydrogen atom to be located in the center. In fact, two minima were obtained with PM7, which differed 19.75 kJ mol^{-1} in energy. The structural differences were marginal though; the O···H distances and O···H···O angle were virtually identical. The only minor difference was the position of the hydrogen atom perpendicular to the O···O axis. The C1–C3–O7–H dihedral angle was 0.98° in one case, and 0.79° in the other. In the PM7 calculations on the dimer reported below, care was taken that the lowest minimum was obtained.

2.2. Dimer

Also for the dimer (see **Figure 2**) the hydrogen bridged form of the monoanion proved to be much more stable than the open form. The difference was 72.5 kJ mol^{-1} for B3LYP and 63.1 kJ mol^{-1} for PM7 (see **Table 2**). Hence, the hydrogen bond appears to be somewhat weaker than in hydrogen succinate, in line with calculations on methyl substituted hydrogen succinates.[22] To obtain further insight into the conformations that the main chain of DIBMA may adopt, the energy of the dimer was calculated as

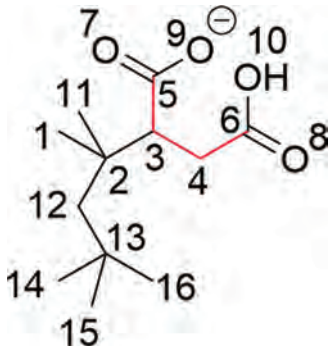

Figure 2. Structure of the dimer with adopted numbering scheme. The important C6C4C3C5 dihedral angle is indicated with red bonds.

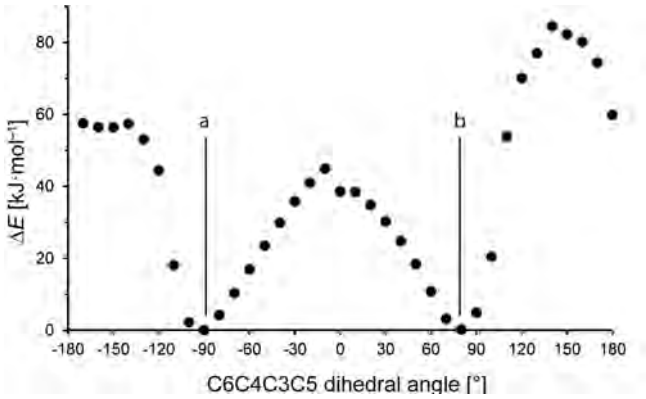

Figure 3. C6C4C3C5 twisting coordinate of the dimer, as obtained from PM7 calculations.

a function of rotation along the C6C4C3C5 and C1C2C3C4 dihedral angles. This was performed in a 10° grid, at the PM7 level of theory, on the 3*S*-enantiomer. Minima were also freely optimized, at both the PM7 and the B3LYP/6-31G** levels of theory.

As shown in **Figure 3**, the C6C4C3C5 twisting coordinate exhibits two minima, one at +80° (minimum b), and one at −90° (minimum a). Free optimizations gave minima at +78.8° and −92.2° for the PM7 method, with the latter minimum being slightly lower in energy (Table 2). With B3LYP/6-31G** comparable results were obtained: minima are situated at +75.7 and −88.7°, the latter conformer being favored by 4.2 kJ mol^{-1}.

In common with hydrogen succinate, in the PM7 calculated structure, the O9···H and O10···H bond lengths and the Mulliken charges on O9 and O10 are highly similar, while the O···H···O angle is again 165–167°. However, some small differences in O···H distances and charges are discernible, which reflect the nonsymmetric structure of the dimer. During the PM7 geometry calculations, the bridging H-atom initially was bonded to O10, but it mostly ended up closer to O9. With DFT again more pronounced differences in the O9···H and O10···H distances and O9 and O10 charges are found, while the O···H···O angle is close to 180°. Note that for both methods the O···O distance is around 2.45 Å.

Thus, analogous to hydrogen succinate, in the DIBMA dimer a short hydrogen bond exists. This hydrogen bond is found to be present for all conformations ranging from −110 to +100°. When it is broken, the energy rises sharply (Figure 3). The energy difference between the minima and the +140° transition state is about 84 kJ mol^{-1}, while the difference between the minima and the maximum at 0° amounts to 45 kJ mol^{-1}. This indicates that the two hydrogen-bonded structures should be able to interconvert, both via the hydrogen-bonded transition state at 0° and at the transition state at +140°, where no hydrogen bond is present. Gas phase calculations on a monoprotonated SMA model compound also revealed a hydrogen-bonded structure. Detailed information on the strength was not provided.[13]

At the transition state at −10° the hydrogen bond is still present, but it is weaker than in the minima. The O···H···O angle is 154.7° instead of the usual 166°, whereas the charges on the oxygen atoms, −0.7948 and −0.7079 for O9 and O10, respectively, differ more than in the other hydrogen-bonded structures. The hydrogen bond is also relatively weak at −110° and +100°. At these dihedral angles, the succinate ring system is just not twisted enough to break the hydrogen bond, but the hydrogen bond is severely under strain. This time this is not expressed in a deviating O···H···O angle, but in different and increased O9···H and O10···H bond lengths, which amount to 1.43 and 1.16 (−110°) and 1.32 and 1.22 Å (+100°), respectively. All in all, there is no minimum in which there is no hydrogen bond in the dimer, showing that it is preferentially maintained. It suggests that the

Table 2. Structural data for minima in the C6C4C3C5 twisting coordinate of the dimer. For atom numbering see Figure 2.

Method	Configu-ration	C6C4C3C5 [°]	Δ *E* [kJ mol^{-1}][a)]	O9–H [Å]	O10–H [Å]	O9–H–O10 [Å]	q O9	q O10	C1C2C3C4 [°]	C11C2C3C4 [°]
PM7	3*S*	−134.1[b)]	72.52		0.98		−0.7523	−0.6087	−171.2	−56.5
B3LYP	3*S*	−154.9[b)]	63.06		0.97		−0.6019	−0.5090	−167.5	−53.1
PM7	3*S*	−92.2	0	1.22	1.26	165.1	−0.7051	−0.7137	180.0	61.5
B3LYP	3*S*	−88.7	0	1.35	1.10	175.0	−0.6307	−0.5633	−176.8	65.1
PM7	3*S*	78.8	0.49	1.23	1.23	167.1	−0.7016	−0.7040	−166.3	76.8
B3LYP	3*S*	75.7	4.18	1.33	1.11	175.9	−0.6331	−0.5798	−166.1	76.9
PM7	3*R*	−80.1	1.26	1.24	1.24	166.7	−0.7061	−0.7006	167.6	−73.8
B3LYP	3*R*	−76.5	2.90	1.33	1.10	175.8	−0.6323	−0.5776	164.8	−77.3
PM7	3*R*	91.0	3.43	1.23	1.25	164.8	−0.7098	−0.7098	−178.2	−58.6
B3LYP	3*R*	87.4	4.43	1.37	1.09	174.5	−0.6306	−0.5623	178.1	−63.3

[a)] Relative to the energy of the −90° conformation of the 3*S* isomer. The energy of this conformation was −1164.76 kJ mol^{-1} (−0.44363236 Hartree) for PM7 and −2024138.11 kJ mol^{-1} (−770.95349019 Hartree) for the B3LYP/6-31G** method; [b)] Open form without hydrogen bond.

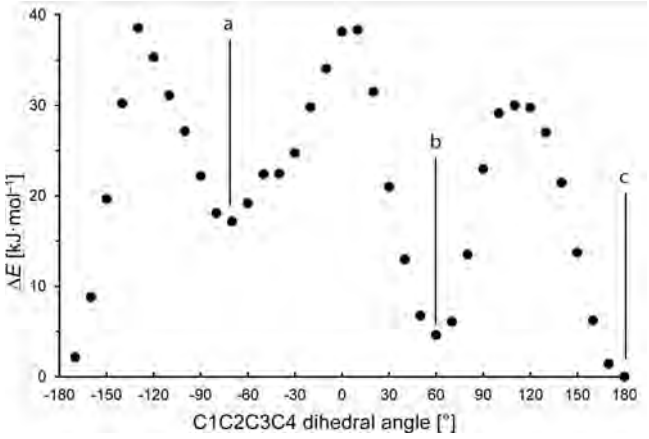

Figure 4. C1C2C3C4 twisting coordinate of the dimer, as obtained from PM7 calculations

structure of DIBMA will be governed by strong hydrogen bonds between the oxygen atoms of the succinate moieties.

The minima were also calculated for the 3*R* configuration of the dimer (Table 2). Not surprisingly, these minima possess similar (though not exactly mirror image) characteristics as 3*S* structures. While for the 3*S* isomers minima were found near +75° and −90°, for the 3*R* structures they occur at −76 to −80° and near +90°. Energies are neither identical. In particular the energy differences between the ± 90° conformations of the *R*- and *S*-enantiomers, 3.4 to 4.4 kJ mol^{-1}, are on the high side. It is of interest to note that the use of stricter convergence criteria and optimization from other starting geometries did not improve this.

In the −90° structures of the 3*S* enantiomers the C1C2C3C4 and C11C2C3C4 dihedral angles amount to −177 to 180° and 61 to 65°, respectively, which are the expected antiperiplanar and synclinal (gauche) conformations for a hydrocarbon chain. In the +75° structures, with values of −166 and 77° these dihedral angles deviate somewhat from the typical values. In order to get more insight into the chain conformation, a conformational analysis was also performed for the C1C2C3C4 twisting coordinate, which functions as a model for the DIBMA backbone. The PM7 calculated coordinate for the 3*S* enantiomer is shown in **Figure 4**. Data for the freely optimized minima obtained with the two different calculation methods are listed in **Table 3**. The coordinate was calculated with C6C4C3C5 dihedral angles of ca −90°, as these minima were seen above to be slightly more stable than those at +75° ones.

It is seen that minima are located near 180 (minimum c), −70 (minimum a) and +60° (minimum b), which are the expected antiperiplanar and gauche conformations. The location of the minima varies with a few degrees for the two methods (Table 3). The antiperiplanar conformation possesses the lowest energy. Note that in this structure the neopentyl side chain, which is much more bulky than the two methyl groups, is in a gauche position with respect to the C3–C4 bond, which forms part of the DIBMA main chain. The +60° conformation is slightly higher in energy. Here the neopentyl group adopts an antiperiplanar position. With PM7 the −70° structure is calculated to have a substantially higher energy, while for the DFT methods it is comparable to the other gauche minimum. The transition states are situated at −130, 10, and 110°, close to the classic anticlinal and synperiplanar angles. They have energies of 30–38 kJ mol^{-1}, meaning that interconversion between the different conformers is possible, and suggesting that the isobutylene part of the DIBMA main chain is rather flexible.

The hydrogen bond is maintained at all C1C2C3C4 dihedral angles. For all minima in the C1C2C3C4 coordinate, the C6C4C3C5 dihedral angle was close to −90°, indicating that there is no strain in the hydrogen succinate part of the molecule, otherwise the energy of the three minima would not have been that similar. The same is true for the other points in the twisting coordinate in Figure 4. The C6C4C3C5 dihedral angle is always close to −90°, except at C1C2C3C4 angles of −20 to 0 and 90°, where it amounts to ca. −68° (data not shown), possibly reducing steric strain between the succinate ring and the alkyl groups. In any case, the hydrogen bond is likely to be maintained during conformational interconversion, as was deduced previously for hydrogen succinate conformer interconversion.[22]

2.3. Trimer

The trimer consists of two diisobutylene units and a single hydrogen succinate ring (**Figure 5**). In this model compound, the diisobutylene unit at the right was appended with a second methyl group to substitute for the next carbon atom in the DIBMA polymer chain. In this way, the trimer contains two chiral atoms, carbon atoms 3 and 4. This gives rise to four stereoisomers, but as each stereoisomer exhibits a minimum at both a negative and a positive C6C4C3C5 dihedral angle, 8 structures are possible.

Results at the B3LYP/6-31G** level of theory are compiled in **Table 4**. It is seen that the lowest energy is found for the 3*S*4*R* isomer with a C6C4C3C5 dihedral angle of 74.5°, similar to one

Table 3. Structural data for minima in the C1C2C3C4 twisting coordinate of the dimer (3*S* configuration). For atom numbering see Figure 2.

Method	C1C2C3C4 [°]	Δ *E* [kJ mol^{-1}][a)]	O9-H [Å]	O10-H [Å]	O9-H-O10 [°]	C6C4C3C5 [°]
PM7	180.0	0	1.22	1.26	165.1	–92.2
B3LYP	–176.8	0	1.35	1.10	175.0	–88.7
PM7	59.6	4.63	1.24	1.24	167.1	–91.0
B3LYP	63.7	1.22	1.38	1.08	174.6	–86.8
PM7	–73.1	16.80	1.24	1.24	164.9	–90.6
B3LYP	–67.0	4.52	1.39	1.07	174.7	–87.2

[a)] Relative to the energy of the antiperiplanar conformation. The energy for this conformation was –1164.76 kJ mol^{-1} (–0.44363236 Hartree) for PM7 and –2024138.11 kJ mol^{-1} (–770.95349019 Hartree) for the B3LYP/6-31G** method.

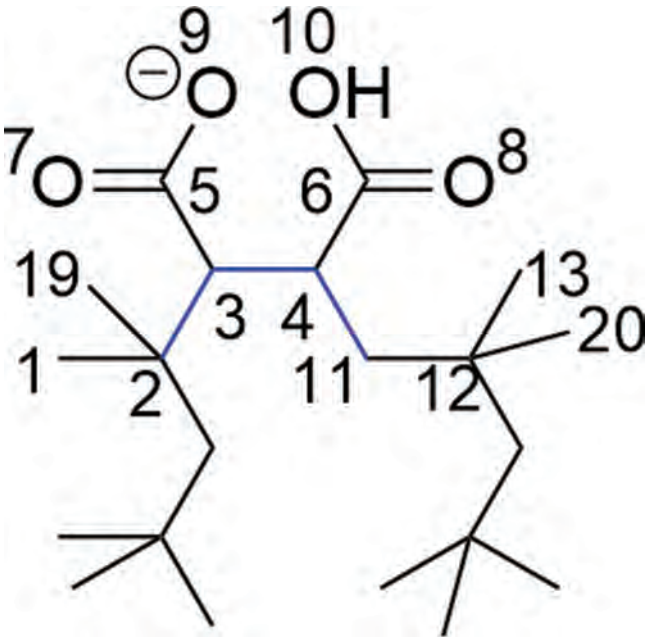

Figure 5. Structure of the trimer with adopted numbering scheme. The C2C3C4C11 dihedral angle is indicated by blue bonds in this figure.

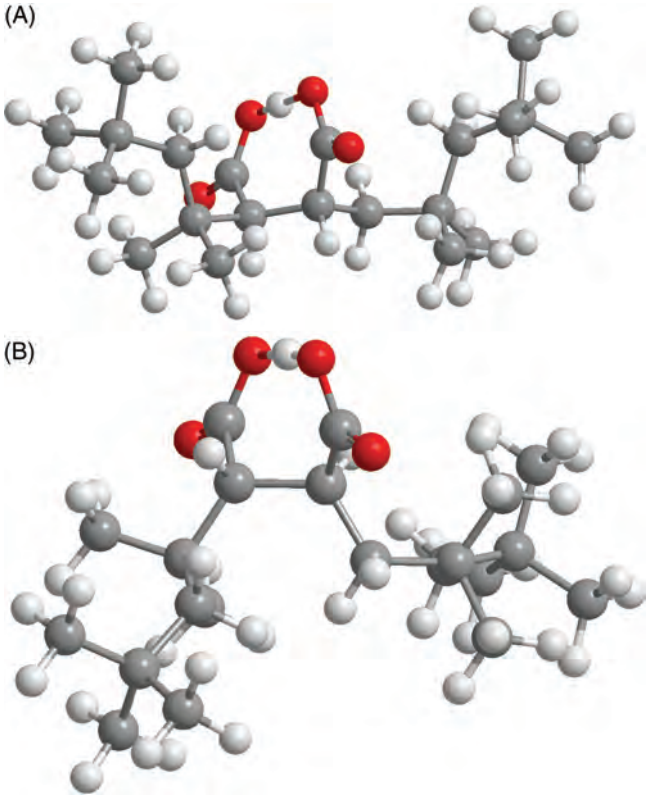

Figure 6. Lowest (3*S*4*R*, C6C4C3C5 = 74.5°, top) and highest (3*R*4*S*, C6C4C3C5 = 97.3°, bottom) energy structures of the trimer.

of the angles found at the minima of the dimer. Its mirror image isomer is the 3*R*4*S* structure with a dihedral angle of −75.6°, which is 5.0 kJ mol^{-1} higher in energy. This is on the high side, and it is seen in Table 4 that there are some minor differences in the various dihedral angles of the two structures. All dihedral angles along the backbone (C1C2C3C4, C2C3C4C11, C3C4C11C12, C4C11C12C13) are in the antiperiplanar range for both structures, though. This undoubtedly is responsible for the low energy of these structures, as the alkyl groups at the C3 and C4 carbon atoms (which form the main chain in the polymer) point away from each other (**Figure 6**). The neopentyl side chains adopt a gauche position with respect to the main chain direction.

In the other minimum of the 3*S*4*R* and 3*R*4*S* enantiomers, the dihedral angles amount to −95.7 and 97.3°, respectively. The energy is much higher than for the ±75° angles, by some 43 kJ mol^{-1}, while the dihedral angle is somewhat larger than the one found for the 3*S* and 3*R* dimers (ca. 88°). The C2C3C4C11 dihedral angle is in a synperiplanar conformation, and the two bulky neopentyl groups are situated on the same side of the hydrogen succinate ring. Hence, in maintaining the hydrogen-bonded ring structure, the C2C3C4C11 dihedral angle is forced into an unfavorable conformation (Figure 6). The energy penalty is still less than rupture of the hydrogen bond would cost.

The 3*R*4*R*/3*S*4*S* enantiomeric pair exhibits minima which are much closer in energy, and which are intermediate in between those of the 3*S*4*R*/3*R*4*S* pair. There is a minimum of +10.4 to +10.5 kJ mol^{-1} with C6C4C3C5 dihedral angles of ca. ±88°, and one of +15.2 to +17.6 kJ mol^{-1} with C6C4C3C5 dihedral angles of ca. ±82°. The C2C3C4C11 dihedral angle belonging to these structures is ca. 90°, also intermediate between those of the *RS* isomers.

Table 4. Structural data for different stereoisomers of the trimer. For atom numbering see Figure 5.

C3	C4	Δ *E* [kJ mol^{-1}][a)]	C6C4C3C5	O9-H [Å]	O10-H [Å]	O9-H-O10 [°]	C1C2C3C4 [°]	C2C3C4C11 [°]	C3C4C11C12 [°]	C4C11C12C13 [°]
R	*S*	5.02	−75.6	1.10	1.34	177.2	162.1	−175.2	176.0	−167.1
S	*R*	42.92	−95.7	1.09	1.36	174.2	−171.0	2.4	−142.3	−176.7
R	*R*	17.58	−83.9	1.10	1.36	176.3	162.0	−84.4	−133.2	−177.9
S	*S*	10.44	−87.9	1.33	1.11	175.8	−170.7	−96.0	179.9	−167.4
R	*S*	43.78	97.3	1.37	1.09	174.1	175.2	1.2	143.7	169.0
S	*R*	0.00	74.5	1.09	1.36	176.6	−160.3	172.0	−172.6	158.6
R	*R*	10.49	89.1	1.10	1.35	175.2	174.7	95.9	−177.8	159.1
S	*S*	15.23	81.5	1.28	1.15	175.2	−159.8	80.6	135.8	169.9

[a)] Relative to the energy of the 3*S*4*R* structure. The calculated energy of this structure was −2953126.50 kJ mol^{-1} (−1124.7864794 Hartree).

Table 5. Structural data for different stereoisomers of the tetramer. For atom numbering see Figure 7.

C3	C4	C12	C13	Δ *E* [kJ mol^{-1}][a)]	C6C4 C3C5 [°]	C16C14 C13C15 [°]	O9-H [Å]	O10-H [Å]	O9-H-O10 [°]	O19-H [Å]	O20-H [Å]	O19-H-O20 [°]	C1C2 C3C4 [°]	C2C3 C4C11 [°]	C3C4 C11C12 [°]	C4C11 C12C13 [°]	C11C12 C13C14 [°]
S	*S*	*S*	*S*	6.04	–88.1	–84.2	1.11	1.34	176.4	1.33	1.11	173.6	–170.3	–96.6	167.0	-154.9	–178.8
R	*S*	*S*	*S*	1.37	–73.9	–83.0	1.08	1.38	175.5	1.10	1.36	172.3	156.0	–170.7	165.5	–161.2	178.3
S	*R*	*S*	*S*	84.89	–94.7	–89.4	1.42	1.06	173.5	1.07	1.40	172.7	–172.3	4.7	–142.1	–68.4	–167.2
S	*S*	*R*	*S*	27.94	–86.4	–86.6	1.36	1.11	176.2	1.37	1.09	174.4	–168.9	–93.5	–176.5	–171.3	–177.3
S	*S*	*S*	*R*	16.65	–90.0	–73.9	1.39	1.08	176.8	1.35	1.10	176.3	–170.3	–98.6	176.3	–49.9	160.5
R	*R*	*S*	*S*	43.23	–87.5	–84.6	1.40	1.08	173.8	1.08	1.39	173.2	158.8	–89.4	–75.2	–128.3	179.8
R	*S*	*R*	*S*	31.11	–74.3	–50.8	1.07	1.39	175.6	1.44	1.05	167.2	155.7	–174.8	138.7	–81.5	–162.0
R	*S*	*S*	*R*	0.00	–74.3	–74.3	1.08	1.38	174.6	1.09	1.36	176.6	156.3	–174.6	153.8	–67.3	161.5

[a)] Relative to the energy of the *RSSR* structure with C6C4C3C5 = –74.3°. The calculated energy of this structure was –4044918.38 kJ mol^{-1} (–1540.628045 hartree).

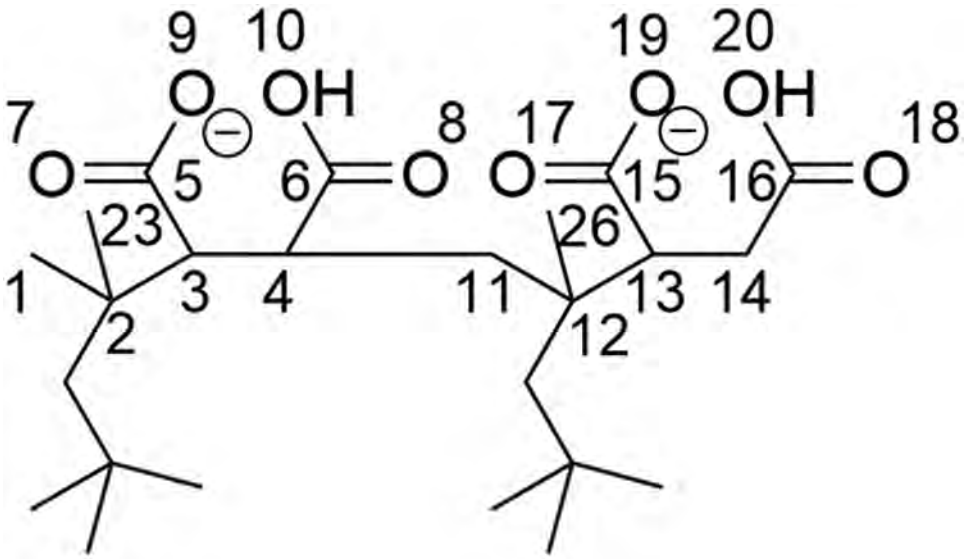

Figure 7. Structure of the tetramer with adopted numbering scheme.

The picture emerges from these trimer calculations that the hydrogen-bonded structure is maintained, and that configurational changes in the C6C4C3C5 region are translated into a change of the C2C3C4C11 dihedral angle. A C6C4C3C5 dihedral angle of 75° is accompanied by an antiperiplanar conformation, a C6C4C3C5 dihedral angle of 95° by a synperiplanar conformation, and a C6C4C3C5 dihedral angle of ca 85° by a near 90°C2C3C4C11 dihedral. Much less variation occurs for the other main chain dihedral angles C1C2C3C4, C3C4C11C12 and C4C11C12C13; they are mostly close to synperiplanar.

It is noteworthy that in the various optimized structures the bridging hydrogen atom seems to be rather arbitrarily found closer to either O9 or O10 (Table 4). The same was true for the tetramer (vide infra, **Table 5**). Hence, there seems to be no systematic relation between the bonding site and some other features. It should be realized that, in comparison to hydrogen succinate, the potential of the coordinate is not strictly symmetric because of the presence of different substituents at C3 and C4. The present findings seem to be in contrast with the behavior of alternating short model compounds for SMA, for which a preference for bonding to one of the oxygen atoms in the hydrogen succinate moiety was reported.[13] However, as the electronic properties of a phenyl substituent (e.g., the polarizability) are much different from that of a neopentyl substituent, it might well be that the preference is smaller for DIBMA model compounds, where conformational changes may already result in a different position of the hydrogen.

2.4. Tetramer

The tetramer contains four chiral atoms, the carbon atoms 3, 4, 12, and 13 (**Figure 7**). This implies that 16 stereoisomers exist. All of these stereoisomers will possess four energy minima: for both positive and negative dihedral angles of the two hydrogen succinate units. Rather than to evaluate all these 64 structures, trends exhibited by the systematic series are focused on in the following.

First the structures of 8 stereoisomers were calculated, with two negative dihedral angles (Table 5). Starting with the struc-

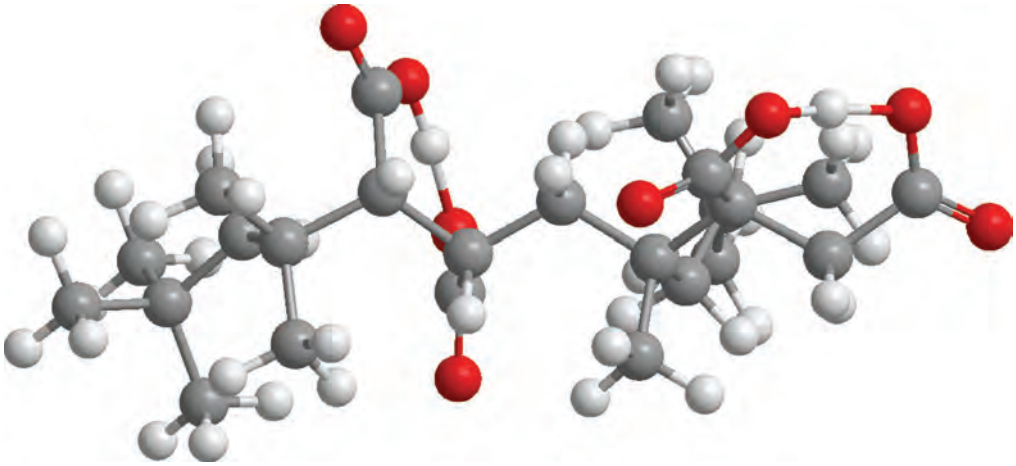

Figure 8. Calculated extended structure of the *RSSS* stereoisomer of the tetramer.

Table 6. Structural data for positive and negative values of the C6C4C3C5 dihedral angle of two stereoisomers of the tetramer. For atom numbering see Figure 7.

C3	C4	C12	C13	Δ *E* [kJ mol^{-1}][a)]	C6C4 C3C5 [°]	C16C14 C13C15 [°]	O9-H [Å]	O10-H [Å]	O9-H-O10 [°]	O19-H (Å)	O20-H (Å)	O19-H-O20 [°]	C1C2 C3C4 [°]	C2C3 C4C11 [°]	C3C4 C11C12 [°]	C4C11 C12C13 [°]	C11C12 C13C14 [°]
R	*S*	*S*	*S*	0.00	−73.9	−83.0	1.08	1.38	175.5	1.10	1.36	172.3	156.0	−170.7	165.5	−161.2	178.3
R	*S*	*S*	*S*	44.50	96.5	−83.9	1.35	1.10	174.8	1.29	1.13	174.5	175.3	2.0	131.5	177.2	177.2
R	*S*	*S*	*S*	25.16	−77.5	77.3	1.33	1.11	175.8	1.10	1.35	176.6	158.4	−179.9	136.8	−76.7	−156.8
R	*S*	*S*	*S*	70.84	94.3	75.0	1.34	1.10	174.1	1.10	1.34	177.4	171.9	−1.3	162.8	−137.4	−159.2
S	*R*	*S*	*R*	31.41	78.3	84.2	1.41	1.07	173.0	1.30	1.13	174.6	−160.0	−179.0	−81.3	−68.3	−177.8
S	*R*	*S*	*R*	45.41	−98.8	86.3	1.44	1.07	172.6	1.36	1.09	174.6	−167.3	−5.7	−156.3	−176.5	−179.4
S	*R*	*S*	*R*	33.60	75.9	−74.4	1.40	1.07	172.3	1.10	1.34	177.6	−159.4	174.9	−116.7	−64.4	152.2
S	*R*	*S*	*R*	85.23	−101.3	−75.5	1.52	1.04	171.0	1.10	1.34	178.0	−168.5	−7.3	−121.7	−60.9	151.5

[a)] Relative to the energy of the *RSSS* structure with C6C4C3C5 = −73.9° and C16C14C13C15 = −83.0°. The calculated energy of this structure was −4044917.01 kJ mol^{-1} (−1540.627525 hartree).

ture with *S* configurations only, gradually *R* configurations are introduced. It is reasonable to assume that the 8 enantiomeric compounds of the calculated structures will give the same results (with an opposite dihedral angle when required).

The lowest energy is found for the *RSSR* structure (ΔH_f = −1540.628045 hartree). This structure is characterized by a dihedral angle of −74.3° for both C6C4C3C5 and C16C14C13C15. Furthermore, four of the five dihedral angles along the molecular backbone are essentially antiperiplanar. The fifth main chain dihedral, C4C11C12C13, is gauche but the neopentyl group at C12 is in an antiperiplanar position with respect to the main chain. This gives an extended structure with a gauche kink for this lowest energy stereoisomer. The structure *RSSS* is very close in energy (+1.37 kJ mol^{-1}). The dihedral angles of C6C4C3C5 and C16C14C13C15 are −73.9 and −83.0°, respectively. All dihedrals in the main chain are essentially antiperiplanar, so that this isomer possesses an extended structure (**Figure 8**). The neopentyl side chains adopt a gauche position.

Although the structures of the tetramers are more complex and elaborate than those of the trimer, the C2C3C4C11 angle still appears to be dominant for the energy. It is seen from Table 5 that structures of low energy have an antiperiplanar C2C3C4C11 angle (and −96.6° in case of *SSSS*), structures of intermediate energy have a C2C3C4C11 angle of about −90°, while the structure of high energy (*SRSS*) has a synperiplanar dihedral angle. This has again its origin in the stereochemistry of the C3 and C4 atoms. An antiperiplanar geometry is found for 3*R*4*S*, a synperiplanar one for 3*S*4*R* (for another example, see the data for structure *SRSR* with C2C3C4C11 = −101.3° and C16C14C13C15 = −75.5° in **Table 6**) while 3*S*4*S* and 3*R*4*R* structures have C2C3C4C11 dihedral angles of about −90°. The C3 and C4 stereochemistry also comes to expression in the magnitude of the C6C4C3C5 dihedral. It is about −75° for 3*R*4*S*, −86 to −90° for 3*S*4*S* and 3*R*4*R*, and −95° for 3*S*4*R*. Hence, in common with the trimer, a dihedral angle of −75° is accompanied by an antiperiplanar conformation of C2C3C4C11 when the configuration is 3*R*4*S*. When the configuration is 3*S*4*R*, a dihedral angle of −95° and a synperiplanar conformation are found. For 3*S*4*S* and 3*R*4*R*, the C6C4C3C5 dihedral is ca. −85°, while the geometry at C2C3C4C11 is orthogonal.

The *SSSS* and *RSRS* isomers fit somewhat less in this picture. The *SSSS* isomer has an orthogonal C2C3C4C11 angle with a

−88° C6C4C3C5 dihedral, but it is low in energy. The main chain has a predominantly all-trans conformation, though. The *RSRS* isomer has a relatively high energy in comparison with the other 3*R*4*S* compounds, but, having a C16C14C13C15 dihedral angle of only −50.8°, here the second hydrogen succinate ring is distorted. With O···H distances of 1.44 and 1.05 Å for O19–H and O20–H, respectively, the hydrogen atom is less shared, while the O···H···O distance is relatively large. Also the O–H–O bond angle of 167.2 is smaller than the usual value in these systems. The environment around C15 looks quite crowded, and it is possible that oxygen atom O19 cannot adopt a position in which it can form a strong hydrogen bond (not shown).

Apart from the −50.8° dihedral angle found for *RSRS*, variation in the geometry near the second H-bonded ring is not very pronounced. The C16C14C13C15 dihedral prefers to adopt a value of −85°, except when the C12 has an *S* and the C13 atom has an *R* configuration. In that case the angle is about −74°. The C11C12C13C14 dihedral angle is close to 180° in all cases.

Next, the effect of introduction of positive values for dihedral angles C6C4C3C5 and C16C14C13C15 was investigated (Table 6). This was done for the isomers *RSSS*, the isomer with the all-trans main chain conformation from Table 5 and *SRSR*, which has the opposite configuration at hydrogen succinate carbons C3, C4, and C13. For *RSSS*, when going from negative to positive C6C4C3C5 dihedral, the energy is raised by 44.50 kJ mol^{-1}. In common with the trimer, it adopts a value of about +95°, while C2C3C4C11 is synperiplanar. When going from negative to positive dihedral at the second hydrogen succinate ring, the increase in energy is 25.16 kJ mol^{-1}, the resulting dihedral value is +77.3°. Now the C4C11C12C13 main chain dihedral, which changes from −161.2 to −76.7°, is affected. When both dihedrals are positive, the total increase in energy is 70.84 kJ mol^{-1}, which more or less equals the sum of the contributions of the two separate effects. Hence, the energy seems to be additive, which suggests that the conformations of the two hydrogen succinate rings behave independently. Note, however, that the C4C11C12C13 dihedral has become −137.4°, which indicates that the structure near the second ring is affected by the geometry of the first ring to some extent. Hence, both in energy and structure the C2C3C4C11 angle seems to be dominant.

In *SRSR*, going from a positive to a negative C6C4C3C5, as expected from the foregoing, increases the strain in the structure, as it is forced in the less favorable −98.8° angle and a synperiplanar C2C3C4C11 conformation. Doing this for C16C14C13C15 has less effect. Despite attaining the more favorable −74.4 dihedral, there is a small increase in energy. When both hydrogen succinate dihedral angles are negative, the energy increases however substantially, by 53.8 kJ mol^{-1}. Clearly, here the effect is not additive. This might be related to the distortion of the hydrogen bond in the first ring, as becomes clear from its −101.3 dihedral angle and the total O···H···O distance of 1.56 Å.

Despite the occurrence of different main chain dihedral angles along the polymer main chain, all tetramers listed in Tables 5 and 6 have an essential elongated structure. Only 3*S*4*R*12*S*13*R* (the compound with the odd −101.3 C6C4C3C5 dihedral) looks to be somewhat curled up. The neopentyl side chains often adopt a gauche conformation with respect to the main chain, but a antiperiplanar orientation with respect to the main chain is also possible, in particular for the side chain at C12.

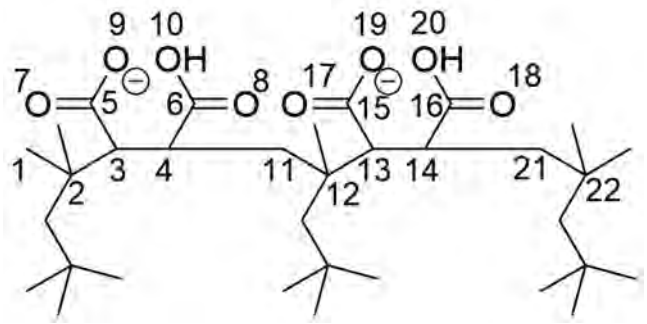

Figure 9. Structure of the pentamer with adopted numbering scheme.

2.5. Pentamer

The structure and numbering of the pentamer are shown in **Figure 9**. We were interested in how the chirality of the carbon atoms affects the structure of the second hydrogen succinate ring. Conformational angles of some of the possible structures with negative dihedrals are given in **Table 7**. The confirmation of the first ring was kept constant at the most stable configuration, i.e., 3*R*4*S*.

Based on the results for the trimer and tetramer, it is expected that a fully antiperiplanar main chain is present when the configuration of atoms C13 and C14 is *R* and *S*, respectively. Indeed, a fully antiperiplanar structure is obtained for the 3*R*4*S*12*R*13*R*14*S* stereoisomer. However, a lower energy is obtained when the configuration at C12 is changed to *S* (Table 7, line 2). In this structure, the C4C11C12C13 dihedral is gauche while the neopentyl side group at C12 is in an position antiperiplanar to the main chain. This is the same situation as obtained for the tetramer, where the lowest energy was obtained for the 3*R*4*S*12*S*13*R* isomer, which also possesses a gauche C4C11C12C13 dihedral and an antiperiplanar neopentyl group (Table 5).

Other results for the second hydrogen succinate ring also are in line with what was derived above for the trimer and tetramer. Thus, when the configuration of the C13 and C14 atoms is identical, the ring adopts a dihedral angle of ca. −90°, while the C12C13C14C21 dihedral is orthogonal. Note that inversion of the C12 stereochemistry now leads to a large increase in energy, despite the C4C11C12C13 angle being gauche again instead of anticlinal (Table 7, lines 3 and 4). For a configuration with C13*S* and C14*R*, the ring dihedral angle is about −95°, while the C12C13C14C21 dihedral is synperiplanar.

The results for the second ring appear to be consistent with those found for the first ring. It may therefore be expected that what has been found for these rings in the trimer, tetramer, and pentamer also holds for all hydrogen succinate rings in a high DIBMA polymer.

3. Discussion

3.1. Hydrogen Bonding in the Repeating Unit

In this contribution, model compounds for the amphiphilic copolymer DIBMA are investigated with PM7 and DFT calculations. These calculations provide a consistent picture for the

Table 7. Structural data for a few stereoisomers of the pentamer. For atom numbering see Figure 9.

C3	C4	C12	C13	C14	Δ *E* [kJ mol^{-1}][a)]	C6C4 C3C5 [°]	C16C14 C13C15 [°]	C1C2 C3C4 [°]	C2C3 C4C11 [°]	C3C4 C11C12 [°]	C4C11 C12C13 [°]	C11C12 C13C14 [°]	C12C13 C14C21 [°]
R	*S*	*R*	*R*	*S*	42.03	−73.8	−71.5	155.3	−170.9	168.8	161.1	−156.6	−168.6
R	*S*	*S*	*R*	*S*	0.00	−73.4	−74.6	155.8	−171.7	169.3	−48.4	161.0	−173.8
R	*S*	*S*	*S*	*S*	28.35	−74.0	−89.9	155.7	−173.2	146.8	−118.5	−175.6	−96.5
R	*S*	*R*	*S*	*S*	84.99	−72.4	−89.0	154.4	−176.6	91.3	−49.6	−159.9	−101.1
R	*S*	*S*	*S*	*R*	39.59	−73.9	−95.9	155.6	−173.1	146.4	−117.7	−177.6	3.0

[a)] Relative to the energy of the *RSSRS* structure. The calculated energy of this structure was −4973900.40 kJ mol^{-1} (−1894.458611 hartree).

different compounds of varying length and yield novel insights into the structure and properties of polymeric DIBMA. The picture that emerges is that the structure of DIBMA is for a large part governed by strong ionic hydrogen bonds within the repeating units. The hydrogen bonds are expected to have a large effect on the structure and properties, and may play a role in the solubilization of lipid bilayers by amphiphilic copolymers of maleic acid.

It should be realized that the data presented here stem from calculations in the gas phase. An important issue is how representative they are for the polymer in aqueous solution, which is the environment where DIBMA exerts its function as a solubilizer of lipid bilayers. In this environment also ions are present, which are neither accounted for in the calculations. They may affect polymer behavior by charge shielding.[31]

The presence of water might severely interfere with the intramolecular hydrogen bonding in the hydrogen succinate moieties. There is little doubt that water molecules solvate the polar groups involved in the hydrogen bond, but it is uncertain whether this solvation is strong enough to disrupt it. In a cluster thermochemistry study it was found that formation of a strongly bonded complex like the acetic acid -acetate dimer ($H_3C–COOH\cdots{}^{-}OOC–CH_3$) from the hydrated separate components is exothermic.[21,32] It was stipulated that in the condensed phase dimer formation was still favorable by about 50 kJ mol^{-1}. MP2/6-31+G* calculations indicated that there was little difference in energy when the acetic acid–acetate dimer was in direct contact or bridged by water molecules.[32] Hence, in the presence of water, the hydrogen bond may continue to exist. An additional indication comes from the alignment of lipid headgroups in bilayers of anionic lipids, in which, e.g., carboxylic acids and carboxylate ions form stable hydrogen-bonded assemblies.[21,32,33]

A factor of interest is that the pK_a values of the two COOH groups in a polymeric succinate unit are distinctively different. For instance, the pK_a values for the first and second deprotonation of SMA with styrene to maleic acid ratios of 1.4:1, 2:1, and 3:1 are 4.4 and 9.0, 5.5 and 8.6, and 5.9 and 8.6, respectively.[11] This suggests that the monoprotonated form is highly stabilized, possibly as a consequence of hydrogen bonding.[34] As far as we aware, pK_a data have not been reported for DIBMA. Two-step deprotonation has been identified in a potentiometric titration in the presence of $CaCl_2$, but pK_a values were not reported.[1] However, for the related copolymer of maleic acid and isobutylene, poly(isobutylenemaleic acid), pK_a values of 3.05 and 9.3 have been measured,[35] strongly suggesting that in DIBMA also a large difference between the two pK_a values exists.

The occurrence of hydrogen bonding in monoprotonated succinate derivatives has been the subject of a long debate. The presence of two different pK_a values is expected for statistical reasons and as a consequence of electrostatic factors. The former leads to a ratio of 4 between the dissociation constants of the first and second deprotonation.[36,37] The second reason is rooted in the negative charge of the monoanion, which makes loss of a positive second proton less probable. Through-bond electronic effects also may play a role.[36]

For hydrogen succinate, it has been deduced from NMR coupling constants that internal hydrogen bonding does not occur in aqueous environment.[37] This was based on the limited change in the percentage of gauche conformers when going from the diprotonated to the monoprotonated state, while it was assumed that the hydrogen-bonded state should have a high preference for a gauche conformation. In later work by the same group, it was shown that in nonprotic solvents hydrogen bonding prevails.[29]

It is of interest that the two-step dissociation process in succinic acid derivatives is strongly affected by the number and size of alkyl substituents. Already in 1939, ΔpK_a was found to vary from 0.84 in succinic acid to 1.6 in dimethylsuccinic acid, 2.3 in diethylsuccinic acid, and 4.2 in tetramethylsuccinic acid.[36] For racemic di-*t*-butyl succinic acid, the widely different pK_a values of 3.6 and 10.2 have been reported.[28,33] It has furthermore been shown that the hydrogen bonding depends on the presence of methyl substituents and the conformational behavior of hydrogen succinate.[30] For copolymers of maleic acid and alkenes, the same situation occurs. While it was already described above that poly(isobutylenemaleic acid) possesses the two widely varying pK_a values of 3.05 and 9.3, for copolymers of maleic acid with *n*-alkenes, which possess a single side chain, differences between the two pK_a values are much smaller.[1] Substituents, like present in SMA and DIBMA, thus have a large effect on the two pK_a values.

The occurrence of two distinct deprotonation steps in copolymers of maleic acid has been related to the polymer chain conformation and the polymer aggregation state.[1,12] Given that the effect is also observed for monomeric succinate derivatives, it is clear that it is not a property exclusive to polymers. Neither can electrostatic and statistical factors alone account for the two-step process, as the presence of two bulky side groups is essential for a large ΔpK_a.

For poly(isobutylenemaleic acid), the two step dissociation process has been described in terms of both short-range and long-range electrostatic interactions in a linear Isling model. The experimental results could only be satisfactory reproduced when low dielectric constants and/or hydrogen bonding (with a modest strength of 21 kJ mol^{-1}) were taken into account.[35] Also for molecular succinic acids, a model was put forward in which alkyl substituents favor the formation of a hydrophobic cavity of low dielectric constant.[36] In such a cavity the hydrogen bond is not disrupted by water, which nicely matches the linear Isling model. The greater size of the alkyl substituents in DIBMA suggests that the hydrogen bond is better shielded from water; the structures depicted in Figures 6 and 8 indeed suggest that the neopentyl substituents shield the hydrogen succinate moieties from the aqueous environment to some extent. Additionally, in water, the polymer may adopt another conformation with a larger hydrophobic space. Aggregation also might play a role.

It has also been argued that the large ΔpK_a in hydrogen di-*tert*-butylsuccinate does not arise from the H-bond itself, but is the consequence of electrostatic repulsion between the carboxylate anions, which is relieved by the presence of a proton in the region between them.[24,28] I.e., the large substituents force the molecule into a conformation in which the two carboxylate groups are in each others vicinity and repel each other, but the repulsion is relieved by the presence of a proton. The C6C4C3C5 torsion angles in several X-rays structures of di-*tert*-butylsuccinate are mostly 70–74°,[28] close to the angles obtained in this contribution, which indicates that there is no real difference between the monomeric and polymeric systems. Hence, irrespective of its exact nature, the observation of a large ΔpK_a for both molecular and polymeric hydrogen succinate derivatives with bulky substituents thus renders it highly likely that the hydrogen bond is present in DIBMA in aqueous environment. Formation of the hydrogen bond might also explain the tolerance of DIBMA to calcium ions,[3,38] as the carboxylate groups are less available for chelation. This high tolerance in comparison to SMA might parallel the larger ΔpK_a values reported for DIBMA-like substances than for SMA (vide supra). The other way around, the tolerance to calcium ions can be taken as an indication that the hydrogen bond is present in water.

Entropy contributions have not been considered so far. Because of loss of rotational freedom, the entropy change associated with hydrogen bond formation will be positive. For hydrogen succinate, the contribution of entropy to the free energy has been estimated as +10 kJ mol^{-1},[37] which is minor in comparison to the enthalpy effect. Moreover, breaking of the hydrogen bond by water molecules and the solvation of the resulting anion and hydroxyl group will be accompanied by a loss of entropy of water, leading to an overall negative free energy change.[32]

Finally, it should not be overlooked that intramolecular H-bond formation in DIBMA is also possible via another motif. They can also be formed between COOH and COO^- groups of neighboring hydrogen succinate units, via a nine-membered ring system. A comparison between the heats of formation of cyclic and linear hydrogen adipate reveals that in this case the H-bonded form is more stable by 103 kJ mol^{-1} (B3LYP/6-31G**), even more than in the case of hydrogen succinate. For the short model compounds under consideration here this will not be of too much importance, as formation of a nine-membered ring goes at the expense of two seven-membered hydrogen bonded rings. However, for a high polymer loss of a succinate hydrogen bond will be outweighed by formation of the adipate hydrogen bond. The occurrence of two different types of hydrogen bonds may impart even more structural rigidity to DIBMA (vide infra). Finally, the formation of intermolecular hydrogen bonds, which induce aggregate formation, also is an option.

3.2. Backbone Structure

The presence of the ionic hydrogen bonds has consequences for the structure of DIBMA with monoprotonated repeating units. The two hydrogen-bonded minima in Figure 3 have a very similar energy so that both of them will be populated. As the barrier is not too high, interconversion between them is well possible at room temperature, as has also been reported for hydrogen succinate.[22] This does however not prevent that there is limited chain flexibility at the hydrogen succinate rings, the more so as the walls of the potential well near −120 and 120° are rather steep. As a consequence of the hydrogen bonding, DIBMA therefore is stiffer than anticipated at first sight.[13,39]

The usual antiperiplanar and gauche dihedral angles are found for the other dihedrals along the DIBMA backbone (Figure 4, Tables 2–7). The barriers are also easily surpassed, making DIBMA dynamically flexible.[40] Based on the conformational properties of the model compounds, DIBMA can thus be regarded as a polymer consisting of semi-rigid hydrogen succinate moieties linked by flexible hydrocarbon parts. In absence of interactions with other chains or ions, DIBMA will thus behave as a random coil polymer, but the repeating unit is quite rigid.[41,12] Bjørnestad et al.[42] recently described that SMA 3:1 adopts a fuzzy globular-shaped aggregate, due to the presence of styrene-rich blocks. It should not be overlooked that in SMA π–π interactions between the styrene pendant groups may play a role. For DIBMA, which is a perfect 1:1 alternating polymer and does not have polarizable side groups, the adoption of such a fuzzy globular aggregate is not likely to occur. Despite the occurrence of different main chain dihedral angles, most DIBMA model compounds have an elongated structure. This might be beneficial for membrane solubilization, as it exposes the hydrophobic tails and renders them available for insertion into the membrane core.

Although antiperiplanar and gauche dihedral angles dominate, 90° and 0° dihedral angles are also found, in particular for C2C3C4C11 (and also for C12C13C14C21). This appears to be related to the stereochemistry of the C3 and C4 atoms. For a negative C6C4C3C5 dihedral angle, the 3*R*4*S* stereochemistry allows an antiperiplanar dihedral angle for C2C3C4C11, whereas this dihedral angle is forced into an unfavorable synperiplanar conformation for the 3*S*4*R* isomer. For both the 3*R*4*R* and 3*S*4*S* isomers a 90° dihedral angle is found. The dihedral angles are imposed by the presence of the hydrogen bond, as can be seen in **Figure 10**. The hydrogen bond dictates a C6C4C3C5 dihedral angle of 75–90°, which leaves C2C3C4C11 dihedral angles of about 180, 0, and 90° for the 3*S*4*R*, 3*R*4*S* and 3*S*4*S* configurations, respectively. Much less variation is found for the other main chain dihedral angles C1C2C3C4, C3C4C11C12, C4C11C12C13, and C11C12C13C14. Hence, C2C3C4C11 (and C12C13C14C21) are dominant in determining the energy and conformation of the polymer chain, which is determined by a combination of the

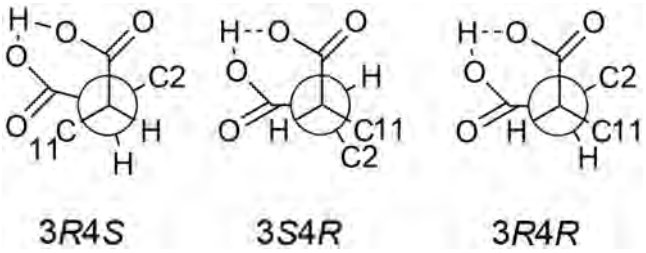

Figure 10. Newman projections along the C4–C3 bond for structures with the 3*R*4*S* (left), 3*S*4*R* (middle) and 3*R*4*R* (right) configurations with negative C6C4C3C5 dihedral angle. It is seen that, by adopting a near-orthogonal geometry, the hydrogen bond forces the structures in antiperiplanar, synperiplanar and orthogonal geometries, respectively.

hydrogen bonding pattern and the configuration of the carbon atoms.

The question then is whether there is a preference for formation of the lowest energy backbone structure. DIBMA is obtained by radical polymerization, which typically gives random tacticity.[41,43] Although there might be factors at work which can favor a stereospecific radical addition, like the bulkiness of the neopentyl group, there is no knowledge that for DIBMA this is the case, as far as we are aware. Hence, it is to be expected that all sorts of dyad and triad stereochemical sequences are present (the ^{1}H and ^{13}C NMR spectra of DIBMA in the anhydride form are very broad, which indeed gives rise to the idea that all sorts of dyad and triad sequences are present). Also in RAFT polymerization, which becomes increasingly popular in DIBMA preparation,[2] stereoselective polymerization is not expected without special conditions.[44]

3.3. Consequences for Mechanism of SMALPING Action

The present study may give clues as to how amphiphilic copolymers based on hydrolyzed maleic anhydride solubilize lipid bilayers and membranes. As outlined in the introduction a few models for the mode of action of amphiphilic copolymers of maleic acid have been described.

The initial bonding of the amphiphilic polymer to the lipid bilayer surface has not been described in great detail yet, except that it might be driven by a hydrophobic interaction between the nonpolar polymer side chains and the hydrophobic part of the bilayer, and that defects in the bilayer might play a role.[42] However, the lipid head groups form a hydrophilic barrier that the polymer side chains need to overcome. For zwitterionic phospholipids it can easily be envisaged that the polymer binds electrostatically to positive charges at the membrane surface with its carboxylate groups, disrupting the order. However, for anionic lipids, this looks less straightforward. Yet, bilayers composed exclusively of anionic phospholipids are still solubilized by amphiphilic polymers.[15] This occurs even in the absence of salts, which might shield the negative charges.

It is not excluded that hydrogen bonds play a role in bonding of the amphiphilic polymer to the lipid bilayer surface. Conspicuously, in membranes containing anionic phospholipids like phosphatidic acid or phosphatidylserine a ionic hydrogen bonding pattern similar to that in DIBMA and SMA may be present, with comparable strength.[21,32,33] Exchange of hydrogen bonds between polymer and lipids might therefore be possible. This does not occur at the expense of a large amount of enthalpy. As a consequence, intermolecular bonds between phospholipids are broken, so that the membrane is disrupted. In addition, upon loss of the hydrogen bonds the polymer chain becomes more flexible, which is favorable from an entropic point of view. It has been recognized before that competing hydrogen bonds (albeit with positively charged amines) can destabilize intramolecular hydrogen bonds and, hence, the structure of membranes[45,46] and that the succinate groups in SMA interact with lipid head groups,[7,42] possibly by formation of hydrogen bonds.[47] The role of the hydrogen bond in the first steps is also indicated by the fact that formation of nanodiscs is most efficient at intermediate pH for model membranes,[11] where the strong ionic hydrogen bond is present, balancing this bond in the lipid bilayers.

4. Conclusions

The structural calculations on the model compounds of DIBMA show that ionic hydrogen bonding within the hydrogen succinate units is important for the structure and properties of this polymer. Although this concerns calculations for the gas phase, it is likely that the hydrogen bonding persists in aqueous solution, given the large difference in the pK_a values for the first and second deprotonation step for both alkyl substituted succinates and copolymers of maleic acid with hydrophobic substituents. The hydrogen bonding brings about that the main chain is semi-flexible and stiffer than anticipated. It also has the consequence that the chain conformation depends strongly on the stereochemistry of the carbon atoms in the succinate rings, and may be a factor of importance in the mechanism of membrane solubilization by maleic acid-based amphiphilic polymers.

5. Experimental Section

Calculations were run with Gaussian 16, Revision A.03[48] such as implemented on the SURFsara system (www.surfsara.nl) with the B3LYP or ωB97XD functionals and the 6-31G** basis set. Inclusion of diffuse functions in the basis set did not lead to significantly different results in test calculations (except for a substantial longer calculation time) and was not continued.

Torsion coordinates were calculated with the PM7MOPAC version of the PM7 semi-empirical method[49] in Gaussian 16. This method is computationally less expensive, but it takes intermolecular interactions and dispersion forces quite well into account and should in this respect not be inferior to DFT methods.[49,50]

Standard termination criteria were used, unless specified otherwise. Symmetry constraints were not imposed. Hessians were calculated for all conformations of hydrogen succinate and the dimer to establish them as genuine minima.

Acknowledgements

SURFsara (www.surfsara.nl) is gratefully acknowledged for the support in using the Lisa Computer Cluster. The author gratefully acknowledges Adrian Kopf, Martijn Koorengevel and Antoinette Killian (Membrane Biochemistry and Biophysics, Utrecht University) for helpful discussions.

Conflict of Interest

The author declares no conflict of interest.

Data Availability Statement

The data that support the findings of this study are available from the corresponding author upon reasonable request.

Keywords

amphiphilic polymers, DFT calculations, hydrogen bonding, membrane solubilization

Received: July 6, 2022
Revised: August 16, 2022
Published online: September 8, 2022

[1] E. Sauvage, D. A. Amos, B. Antalek, K. M. Schroeder, J. S. Tan, N. Plucktaveesak, R. H. Colby, *J. Polym. Sci., Part B: Polym. Phys.* **2004**, *42*, 3571.
[2] L. E. Ball, L. J. Riley, W. Hadasha, R. Pfukwa, C. J. I. Smith, T. R. Dafforn, B. Klumperman, *Biomacromolecules* **2021**, *22*, 763.
[3] A. O. Oluwole, B. Danielczak, A. Meister, J. O. Babalola, C. Vargas, S. Keller, *Angew. Chem., Int. Ed.* **2017**, *56*, 1919.
[4] T. J. Knowles, R. Finka, C. Smith, Y.-P. Lin, T. Dafforn, M. Overduin, *J. Am. Chem. Soc.* **2009**, *131*, 7484.
[5] J. M. Dörr, S. Scheidelaar, M. C. Koorengevel, J. J. Dominguez, M. Schäfer, C. A. Van Walree, J. A. Killian, *Eur. Biophys. J.* **2016**, *45*, 3.
[6] M. Overduin, B. Klumperman, *Eur. Polym. J.* **2019**, *110*, 63.
[7] M. C. Orwick, P. J. Judge, J. Procek, L. Lindholm, A. Graziadei, A. Engel, G. Gröbner, A. Watts, *Angew. Chem., Int. Ed.* **2012**, *51*, 4653.
[8] M. Jamshad, V. Grimard, I. Idini, T. J. Knowles, M. R. Dowle, N. Schofield, P. Sridhar, Y. Lin, R. Finka, M. Wheatley, O. R. T. Thomas, R. E. Palmer, M. Overduin, C. Govaerts, J.-M. Ruysschaert, K. J. Edler, T. R. Dafforn, *Nano Res.* **2015**, *8*, 774.
[9] D. J. K. Swainsbury, S. Scheidelaar, R. Van Grondelle, J. A. Killian, M. R. Jones, *Angew. Chem., Int. Ed.* **2014**, *53*, 11803.
[10] J. M. Dörr, M. C. Koorengevel, M. Schäfer, A. V. Prokofyev, S. Scheidelaar, E. A. W. Van Der Cruijsen, T. R. Dafforn, M. Baldus, J. A. Killian, *Proc. Natl. Acad. Sci. USA* **2014**, *111*, 18607.
[11] S. Scheidelaar, M. C. Koorengevel, C. A. Van Walree, J. J. Pardo Dominguez, J. M. Dörr, J. A. Killian, *Biophys. J.* **2016**, *111*, 1974.
[12] S. R. Tonge, B. J. Tighe, *Adv. Drug Delivery Rev.* **2001**, *53*, 109.
[13] C. Malardier-Jugroot, T. G. M. Van De Ven, M. A. Whitehead, *J. Phys. Chem. B* **2005**, *109*, 7022.
[14] A. H. Kopf, J. M. Dörr, M. C. Koorengevel, F. Antoniciello, H. Jahn, J. A. Killian, *Biochim. Biophys. Acta, Bioenerg.* **2020**, *1862*, 183125.
[15] S. Scheidelaar, M. C. Koorengevel, J. D. Pardo, J. D. Meeldijk, E. Breukink, J. A. Killian, *Biophys. J.* **2015**, *108*, 279.
[16] M. Xue, L. Cheng, I. Faustino, W. Guo, S. J. Marrink, *Biophys. J.* **2018**, *115*, 494.
[17] M. Orwick Rydmark, M. K. Christensen, E. S. Köksal, I. Kantarci, K. Kustanovich, V. Yantchev, A. Jesorka, I. Gözen, *Soft Matter* **2019**, *15*, 7934.
[18] P. S. Orekhov, M. E. Bozdaganyan, N. Voskoboynikova, A. Y. Mulkidjanian, H.-J. Steinhoff, K. V. Shaitan, *Langmuir* **2019**, *35*, 3748.
[19] J.-D. Chai, M. Head-Gordon, *Phys. Chem. Chem. Phys.* **2008**, *10*, 6615.
[20] A. Li, H. S. Muddana, M. K. Gilson, *J. Chem. Theory Comput.* **2014**, *10*, 1563.
[21] M. Meot-Ner (Mautner), *Chem. Rev.* **2012**, *112*, PR22.
[22] J. Guo, P. M. Tolstoy, B. Koeppe, G. S. Denisov, H.-H. Limbach, *J. Phys. Chem. A* **2011**, *115*, 9828.
[23] J. Emsley, *Chem. Soc. Rev.* **1980**, *9*, 91.
[24] C. L. Perrin, *Acc. Chem. Res.* **2010**, *43*, 1550.
[25] N. Kalsbeek, S. Larsen, *Acta Crystallogr.* **1991**, *C47*, 1005.
[26] P. R. Mallinson, C. S. Frampton, *Acta Crystallogr.* **1992**, *C48*, 1555.
[27] P. Lemoine, N. Dumait, V. Dorcet, S. Cordier, *J. Chem. Crystallogr.* **2020**, *50*, 35.
[28] C. L. Perrin, J. S. Lau, Y.-J. Kim, P. Karri, C. Moore, A. L. Rheingold, *J. Am. Chem. Soc.* **2009**, *131*, 13548.
[29] M. S. Rudner, S. Jeremic, K. A. Petterson, D. R. Kent IV, K. A. Brown, M. D. Drake, W. A. Goddard, J. D. Roberts, *J. Phys. Chem. A* **2005**, *109*, 9076.
[30] J. Guo, P. M. Tolstoy, B. Koeppe, N. S. Golubev, G. S. Denisov, S. N. Smirnov, H.-H. Limbach, *J. Phys. Chem. A* **2012**, *116*, 11180.
[31] Y.-K. Li, M.-W. Jiang, L. Wang, C.-G. Guo, Y. Xu, C.-Q. Wang, *J. Polym. Sci., Part B: Polym. Phys.* **2013**, *51*, 1598.
[32] M. Meot-Ner, D. E. Elmore, S. Scheiner, *J. Am. Chem. Soc.* **1999**, *121*, 7625.
[33] T. H. Haines, *Proc. Natl. Acad. Sci. USA* **1983**, *80*, 160.
[34] D. H. Mcdaniel, H. C. Brown, *Science* **1953**, *118*, 370.
[35] T. Kitano, S. Kawaguchi, N. Anazawa, A. Minakata, *Macromolecules* **1987**, *20*, 2498.
[36] F. H. Westheimer, M. W. Shookhoff, *J. Am. Chem. Soc.* **1939**, *61*, 555.
[37] E. S. Lit, F. K. Mallon, H. Y. Tsai, J. D. Roberts, *J. Am. Chem. Soc.* **1993**, *115*, 9563.
[38] A. H. Kopf, O. Lijding, B. O. W. Elenbaas, M. C. Koorengevel, J. M. Dobruchowska, C. A. Van Walree, J. A. Killian, *Biomacromolecules* **2022**, *23*, 743.
[39] M. Esmaili, C. J. Brown, R. Shaykhutdinov, C. Acevedo-Morantes, Y. L. Wang, H. Wille, R. D. Gandour, S. R. Turner, M. Overduin, *Nanoscale* **2020**, *12*, 16705.
[40] H. R. Allcock, F. W. Lampe, J. E. Mark, *Contemporary Polymer Chemistry*, 3rd ed., Pearson, Upper Saddle River **2003**, Ch. 18.
[41] F. A. Bovey, *Chain Structure and Conformation of Macromolecules*, Academic Press, New York **1982**, Chaps. 3,7.
[42] V. A. Bjørnestad, M. Orwick-Rydmark, R. Lund, *Langmuir* **2021**, *37*, 6178.
[43] A. Matsumoto, in *Handbook of Radical Polymerization* (Eds: K. Matyjaszewski, T. P. Davis), Wiley, Hoboken **2002**, Ch. 13.
[44] M. Kamigaito, K. Satoh, *Macromolecules* **2008**, *41*, 269.
[45] E. E. Kooijman, K. M. Carter, E. G. Van Laar, V. Chupin, K. N. J. Burger, B. De Kruijff, *Biochemistry* **2005**, *44*, 17007.
[46] E. E. Kooijman, D. P. Tieleman, C. Testerink, T. Munnik, D. T. S. Rijkers, K. N. J. Burger, B. De Kruijff, *J. Biol. Chem.* **2007**, *282*, 11356.
[47] S. Banerjee, T. K. Pal, S. K. Guha, *Biochim. Biophys. Acta, Biomembr.* **2012**, *1818*, 537.
[48] M. J. Frisch, G. W. Trucks, H. B. Schlegel, G. E. Scuseria, M. A. Robb, J. R. Cheeseman, G. Scalmani, V. Barone, G. A. Petersson, H. Nakatsuji, X. Li, M. Caricato, A. V. Marenich, J. Bloino, B. G. Janesko, R. Gomperts, B. Mennucci, H. P. Hratchian, J. V. Ortiz, A. F. Izmaylov, J. L. Sonnenberg, D. Williams-Young, F. Ding, F. Lipparini, F. Egidi, J. Goings, B. Peng, A. Petrone, T. Henderson, D. Ranasinghe, et al., Gaussian 16, Revision A.03, Gaussian, Inc., Wallingford CT, **2016**.
[49] J. J. P. Stewart, *J. Mol. Model.* **2013**, *19*, 1.
[50] A. S. Christensen, T. Kubař, Q. Cui, M. Elstner, *Chem. Rev.* **2016**, *116*, 5301.

